



# Structural concrete design by the CFP methodology

M. N. Pavlović<sup>(1)</sup> M. D. Kotsovos<sup>(2)</sup>

#### **Abstract**

The "compressive-force path" (CFP) design methodology is briefly presented as an alternative to some of the current design concepts as embodied in present codes of practice. The methodology is new, and yet it could be said to derive from some of the design approaches from ancient Greek and Roman times. Its physical concept can easily be visualized by structural engineers who will readily understand that a beam behaves more efficiently when

designed as a tied arch and that, when such a stiffer load path is provided, nature will follow it, a fact well known in structural theory. Several examples, covering a wide variety of situations, are also presented, illustrating potentially serious shortcomings in some of the guidelines in current codes of practice.

Keywords: concrete structures; compressive-force path; structural design.

<sup>(1)</sup> Prof. Ph.D. Department of Civil and Environmental Engineering, Imperial College, University of London, London SW7 2AZ, UK. e-mail: m.pavlovic@imperial.ac.uk

<sup>(2)</sup> Prof. Ph.D. Department of Civil Engineering, National Technical University of Athens, Athens 15780, Greece. e-mail: m.kots@civil.ntua.gr

### 1. Introduction

The design of a structural concrete member for ultimate strength requires the availability of methodologies capable of yielding realistic descriptions of the member's ultimate characteristics, such as, for example, flexural capacity, shear capacity, ductility, etc. Current methodologies commonly employed for assessing the ultimate characteristics of a structural concrete member involve the use of analytical formulations which express the strength characteristics as a function of the member geometry and dimensions, as well as the mechanical properties of the materials from which the member is made. An important feature of these analytical formulations is the inclusion in them of empirical parameters, the evaluation of which is essential for the calibration of the formulations, such calibrations being achieved by using experimental data on the strength and deformational characteristics of the member. It is evident, therefore, that the very need to include these empirical parameters implies that the analytical formulations yield predictions which deviate from the corresponding values established by experiment.

Deviations up to approximately 10% are generally considered as natural since they are usually due to the scatter of the experimental data used for the calibration of the semi-empirical

formulations relevant to the design method employed. On the other hand, deviations between approximately 10% and 20% are usually attributed to the lack (or deficiency) of experimental data sufficient to secure a conclusive calibration of the semi-empirical formulations. Deviations larger than 20% should be attributed to the lack of a sound theory underlying the derivation of the semi-empirical analytical formulations. In such a case, a reappraisal of the underlying theory is essential before an attempt is made to improve the prediction by acquiring additional experimental data for the more accurate calibration of the analytical formulations used.

In recent years there have been serious doubts expressed regarding the validity of a number of the fundamental principles (named, with some hyperbole, myths and fallacies) underlying code-based design, and especially earthquake-resistant design (Priestley 1997; Hansford 2002). Many problems with design for shear strength were also identified. However, no doubts were expressed regarding the validity of the truss analogy (TA), which underlies reinforced-concrete (RC) design.

TA, since its inception at the turning to the 20<sup>th</sup> century (Ritter 1899; Mõrsch 1902), has always formed the basis of RC design. It became attractive for its simplicity and was first implemented in

design through the permissible-stress philosophy. With the introduction of the limit-state philosophy, in the mid 1970s, its use was extended for the description of the physical state of RC structures at their *ultimate-limit state* by incorporating concepts such as strain softening (Barnard 1964), aggregate interlock (Fenwick and Pauley 1968; Taylor 1974), dowel action (Taylor 1969), etc. TA has remained to date the backbone of RC design, with more refined versions of it (in the form of the compression-field theory (Collins and Mitchell 1980) and strut-and-tie models (Schlaich et al. 1987)) becoming increasingly popular (Canadian Standards Association 1984; American Concrete Institute 2002).

And yet, the concepts which underlie the implementation of TA in limit-state design are incompatible with fundamental properties of concrete at the material level. For example, strain-softening has been found to describe the interaction between specimen and testing device rather than the post-peak behaviour of concrete (Kotsovos 1983; Van Mier 1986; Van Mier et al. 1997). Similarly, aggregate interlock and dowel action can only be effected through the shearing movement of the crack faces and this is incompatible with the cracking mechanism of concrete which involves crack extension in the direction of the maximum principal compressive stress and crack opening in the orthogonal direction (Kotsovos 1979, Kotsovos and Newman 1981). Moreover, tests on RC beams have shown that the contribution of both aggregate interlock (Kotsovos 1987; Kotsovos and Pavlović 1986, 1995, 1999) and dowel action (Jelic et al. 1999) on the beam load-carrying capacity is, if any, negligible.

## 2. The CFP methodology

In order to address shortcomings in code-design methods, the Authors first developed a nonlinear finite-element model (NLFEM) for structural concrete to provide realistic strength and ductility estimates. Based on true material properties - with triaxial behaviour becoming unavoidable in critical regions of a structure prior to failure - its predictive reliability has been illustrated in detail (Kotsovos and Pavlović 1995) for a wide variety of structural forms: in fact, examples were presented illustrating how certain code predictions of structural strength can result in large margins of error, ranging from 100% overestimates (e.g. structural walls) to 1000% underestimates (e.g. Tbeams). This approach has been described at length elsewhere (Kotsovos and Pavlović 1995; González Vidosa et al. 1991a, b) and will not be further discussed in what follows.

Besides the above formal analytical tool, a second technique (termed the compressiveforce path (CFP) methodology) was also

developed by the Authors. The latter method, which has been described in detail in a text (Kotsovos and Pavlović 1999), represents a lower-level methodology than its NLFEM counterpart; however, despite the fact that it relies on simple hand calculations requiring no more effort than that implicit in checks based on current code provisions, this simplified technique has been shown to yield quite accurate predictions for the case of skeletal structures (or, more generally, those structures which can be approximated by equivalent beams or frames). Such predictions have exposed discrepancies with respect to some code predictions that are as high as 300%-500%, both on the safe and unsafe sides, as will be illustrated later by reference to several problems.

The CFP methodology has its origin in Kani's work (1964). As this was applied in practice (Bobrowski and Bardham-Roy 1984) by Bobrowski and Bardham-Roy (1969) and is fully described elsewhere (Kotsovos and Pavlović 1999), it will be presented in a very concise manner herein. The methodology provides the basis for the implementation of the limit-state philosophy into practical design of reinforced-concrete (RC) structures through:

- identifying the regions that form the path along which the compressive forces developing within a structural element or structure under load are transmitted to the supports;
- strengthening these regions so as to impart on the element or structure

the desired load-carrying capacity and sufficient ductility.

In fact, the use of the name *compressive-force path* has been intended to highlight the above two key features of the methodology.

As an illustrative example of the application of the CFP methodology for the design of RC structural elements, Fig. 1 shows the model considered by this methodology as the most suitable for providing a simplified, yet realistic, description of the physical state of a two-span linear element under the maximum transverse load that it is capable of sustaining at the middle of its larger span combined with a concentric axial load inducing a nominal compressive stress of the order of  $0.2f_c$ . For comparison purposes, the figure also includes the TA for this type of structural member.

The construction of the CFP physical model is based on the bending-moment diagram of the structure. This is true whether one is dealing with a single beam or a multi-element structural system (such as a continuous beam (as in Fig. 1) or a frame). The portions of the structure between consecutive points of zero bending moment are considered as "simply-supported" elements connected at the point of contraflexure, which takes the form of an internal support, as indicated in Fig. 2. Each one of the simply-supported elements is modelled as indicated in Fig. 3, with the internal support (at the location of transverse tension marked as 3 in Fig. 1) being effected by a transverse tie, as it is schematically represented by the tie 22'

in Fig. 2 and tie 3 in Fig. 3. It is interesting to note in Figs. 1 and 3 that, unlike the physical models (invariably based on the TA) incorporated in current codes of practice, the CFP method identifies the locations of the structural element where the development of transverse tension is most likely to cause brittle types of failure (see locations marked with 1 to 6 in Fig. 1 and 3).

With the exception of the direct tensile stresses (marked as 3 in Fig. 1 and 3) developing in the region of the point of contraflexure, the location of tensile stresses developing transversely to the direction of the compressive-force path within each of the simply-supported subelements (shown in Fig. 3) depends on the value of the shear span-to-depth ratio, which affects the beam load-carrying capacity in the manner indicated in Fig. 4 (Kani 1964). In fact, the trends

exhibited by the variation of load-carrying capacity with the shear span-to-depth ratio (a/d) correspond to four distinct types of structural-element behaviour, two of which - types II and III - being characterised by brittle modes of failure, whereas for types I and IV the structural element may be designed to exhibit ductile behaviour without the provision of transverse reinforcement in excess of a nominal amount (Kani 1964). All four types of behaviour are fully quantified by a single analytical expression for the type II behaviour derived from empirical data (Kotsovos and Pavlović 1999) (note that type III behaviour consists of linear interpolation between types IV and III). This expression contains all geometric (and load) parameters (including T-beams, with even an allowance for web tapering) as well as the main-reinforcement characteristics (i.e. reinforcement percentages).

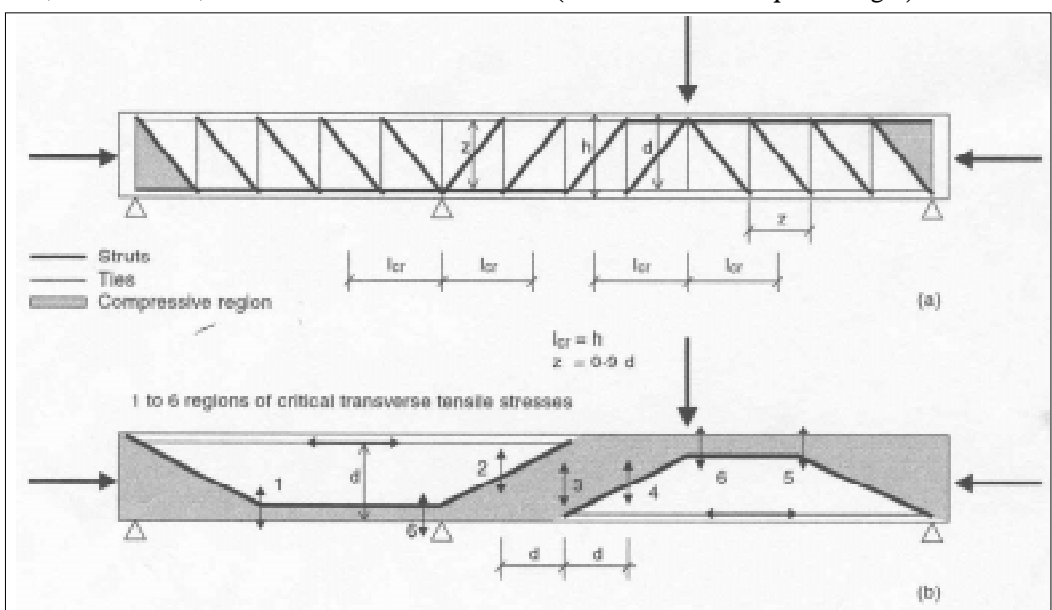


Figure 1: Physical models for a two-span continuous beam based on (a) TA and (b) CFP. (1<sub>cr</sub>: critical lengths as defined in codes - Comité Européen de Normalisation 1991, 1994).

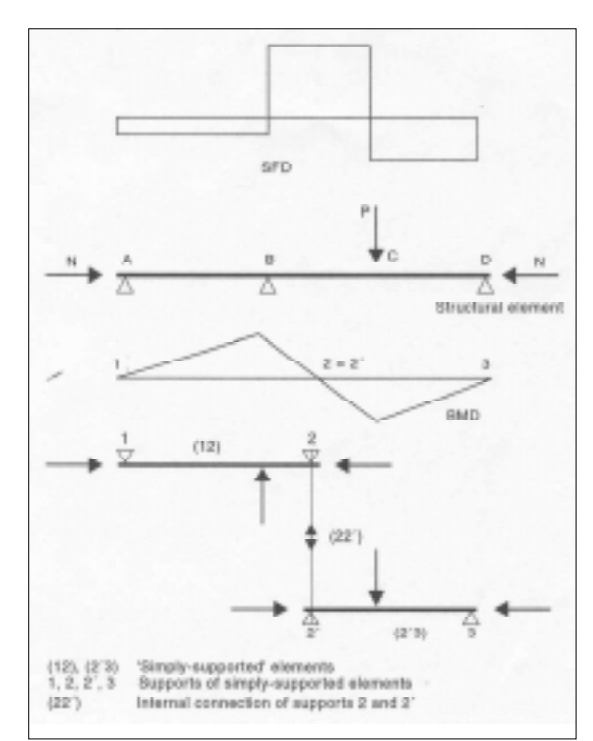


Figure 2: Explanation of how the CFP physical model for the beam in Fig. 1 is constructed. (SFD: shear-force diagram. BMD: bending-moment diagram).

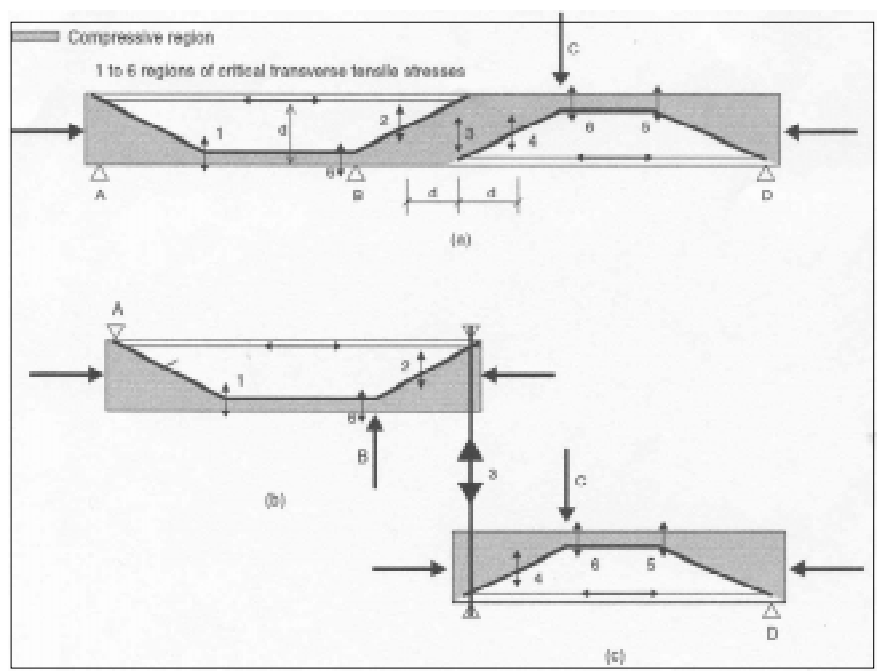


Figure 3: Simply-supported components (b and c) connected by tie 3 of CFP model (a) of the two-span beam shown in Fig. 1.

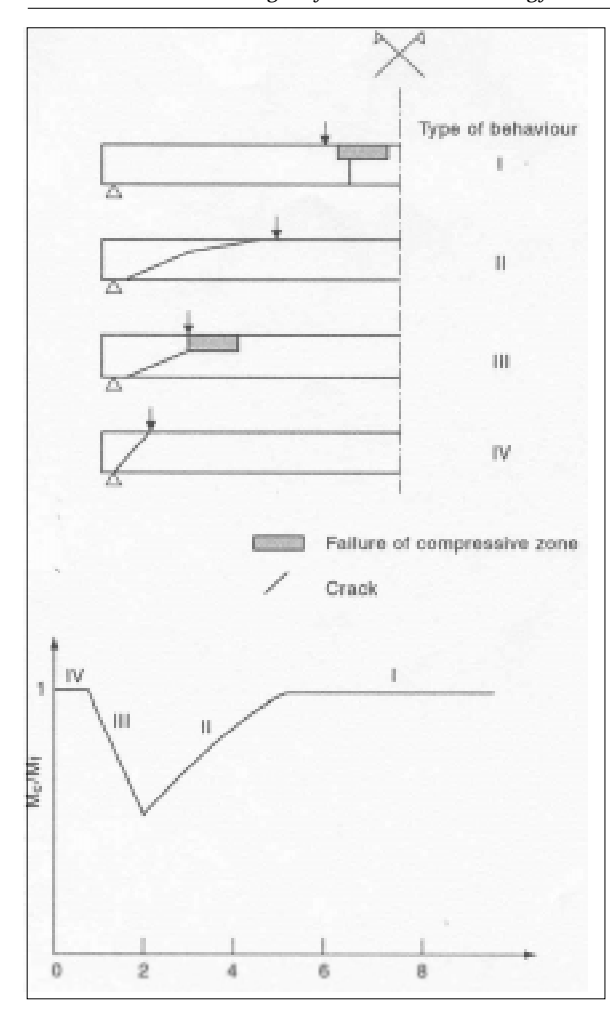


Figure 4: Dependence of load-carrying capacity (expressed as  $M_c/M_p$ ) and type of element behaviour on  $a_v/d$ .  $(M_f$ : flexural capacity;  $M_c$ : bending moment corresponding to load-carrying capacity;  $a_v/d$  = shear-span to - effective - depth ratio).

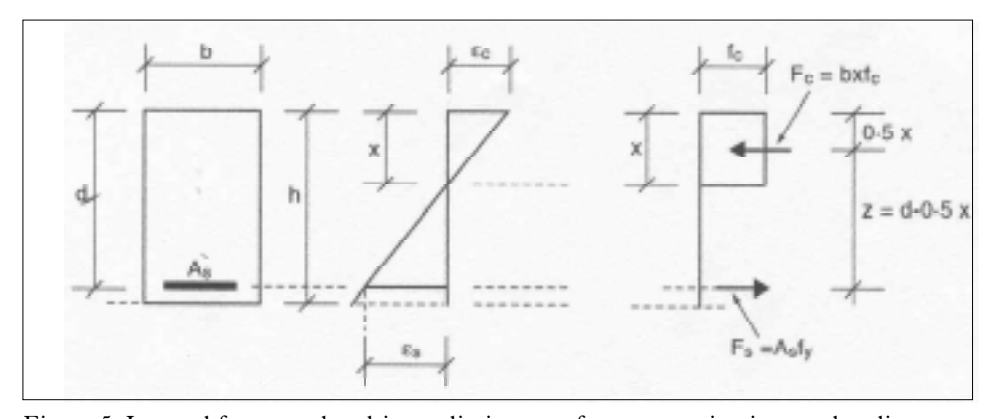


Figure 5: Internal forces at the ultimate-limit state of a cross-section in pure bending.

Type I behaviour is characterized by a flexural mode of failure, which is ductile when flexural capacity is reached, namely when the compressive zone reaches its load-carrying capacity after yielding of the longitudinal reinforcement. Flexural capacity is assessed as indicated in Fig. 5. The figure provides a simplified description of the internal actions at a given crosssection at its flexural capacity, which differ only slightly from those specified by current codes in that the compressive zone is considered to be subjected to a uniform stress equal to  $f_c$  over its full depth x rather than k f over a depth equal to  $\alpha x$  (where k=0.85,  $\alpha=0.8$  in accordance with the EC2 (Comité Européen de Normalisation 1994) and  $f_c$  is the uniaxial (cylinder) compressive strength of concrete).

The brittle mode of failure associated with type II behaviour is caused by tensile stresses developing either in the region of change of the CFP direction (regions 1 and 5 in Figs. 1b and 3) or in the region of the longitudinal member of the frame (regions 6 in Figs. 1b and 3) subjected to the combined action of the maximum bending moment and shear force (see Fig. 2). According to the CFP method, the transverse-stress resultant in the former of the above regions is numerically equal to the acting shear force; sufficient transverse reinforcement is specified to sustain the portion of the shear force in excess of that which can be sustained by concrete alone. Such reinforcement is uniformly distributed within a length equal to the cross-sectional depth (d), symmetrically about the location of the change of the CFP direction. For the remaining portion of the shear span, it is deemed sufficient to place a nominal amount of transverse reinforcement capable of sustaining a transverse tensile stress of the order of 0.5 MPa. In any case, noreinforcement is placed minal throughout the shear span when concrete alone is capable of sustaining the tensile stress in the region of change of the CFP direction.

In the compressive zone of the crosssection subjected to the combined action of the maximum bending moment and shear force (locations 6 in Figs. 1b and 3), transverse tensile stresses may develop due to the loss of bond between the longitudinal reinforcement and the surrounding concrete in the manner indicated in Fig. 6. The figure indicates a portion of the structural element between two cross-sections defined by consecutive cracks, together with the internal forces which develop in these cross- sections before and after the loss of bond  $\tau$ , necessary to develop the increase in tensile force  $\Delta F_s$ . From the figure, it can be seen that the loss of bond may lead to an extension of the right-hand side crack and, hence, a reduction of the compressive zone depth, x, which is essential for the rotational equilibrium of this portion as indicated by the relation

 $F_{\rm s}(x-x_{\rm p})/2=V(x/2)$ . The reduction of the compressive-zone depth increases the intensity of the compressive stress field, as compared to its value at the left-hand side of the portion, thus leading to dilation of the volume of concrete, which causes the development of transverse-tensile stresses ( $\sigma$ , in Fig. 6) in the adjacent regions. Failure may be prevented by placing reinforcement in the form of stirrups: these should be stirrups in the compression zone and distributed across the beam's breadth such as, for example, hoop stirrups and not the usual vertical stirrups running through the beam's depth which would be ineffective (especially in the case of flanges of T-sections). Such stirrups must be placed around the cross-section where the point load acts (see locations 6 in Figs. 1b and 3): for monotonic loading, they should extend a distance d on either side of point loads, while for cyclic loading stirrups ought to extend, additionally, along the horizontal shaded portion of the model (i.e. between locations 1 and 6 at the lefthand side sub-element, and locations 5 and 6 at the right-hand side one – see Fig. 3, as well as Fig. 10 which depicts the reinforcement detailing of the RC twospan linear element shown in Fig. 1). The quantity of the stirrups will be sufficient to sustain the portion of the tensile-stress resultant in excess of that which can be sustained by concrete alone.

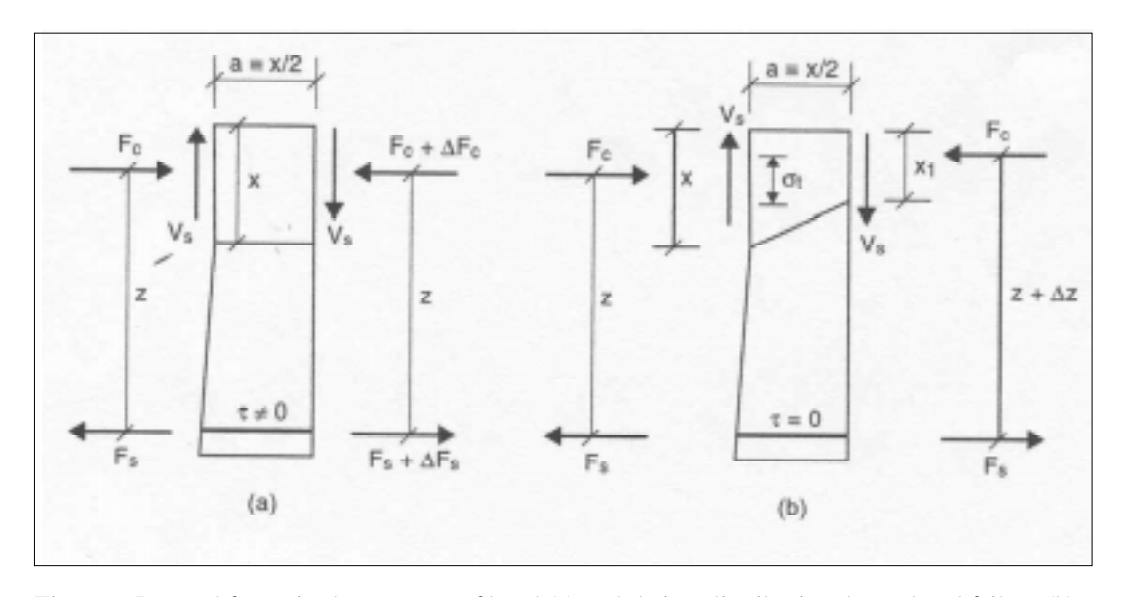


Figure 6: Internal forces in the presence of bond (a) and their redistribution due to bond failure (b).

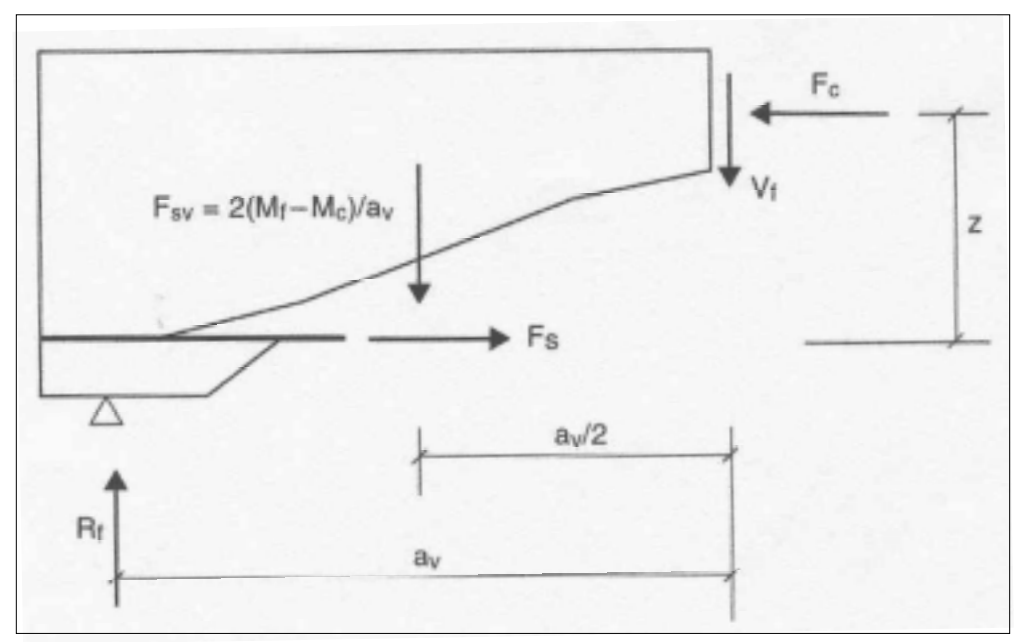


Figure 7: Assessment of transverse reinforcement for structural elements characterised by type III behaviour:  $M_f = R_i \rho_v$  (= flexural capacity of critical section);  $M_c = F_i z$  (=bending moment causing brittle failure);  $F_{sv} = 2(M_f M_v)/a_v$  (=total force sustained by transverse reinforcement); therefore, the total amount of transverse reinforcement (centred around the middle of the shear span as shown in the figure) is  $A_{sv} = F_{sv}/(f_{vv}/g_s)$ .

In contrast with type II behaviour, the brittle failure characterizing type III behaviour is a flexural mode of failure caused by the loss of load-carrying capacity of the compressive zone (the depth of which decreases considerably due to the deep penetration of the inclined crack that forms within the shear span) before yielding of the tension reinforcement. This type of failure is prevented by uniformly distributing transverse reinforcement throughout the shear span in a quantity sufficient to sustain a transverse-tensile force whose moment about the "critical"

cross-section (i.e. the cross-section through the tip of the deep inclined crack) increases the moment capacity of this cross-section beyond its flexural capacity (see Fig. 7). It is important to understand that the function of the stirrups in type II behaviour is not to help carry shear but to provide additional moment capacity.

Type IV behaviour is typical deepbeam behaviour. Although, as indicated in Fig. 4, its load-carrying capacity corresponds to flexural capacity, loss of load-carrying capacity may be attributable to either failure of the compressive zone within the middle portion of the structural element (i.e. failure of the horizontal element of the "frame" of the proposed model) or failure in compression of the inclined end zone of this element (i.e. failure of the inclined leg of the "frame" of the proposed model). In the former case, failure may be ductile (resembling flexural failure) while, in the latter case, it is brittle (resembling uniaxial-compression failure). A simple design method that can be used for predicting both load-carrying capacity and mode of failure is briefly described in Fig. 8.

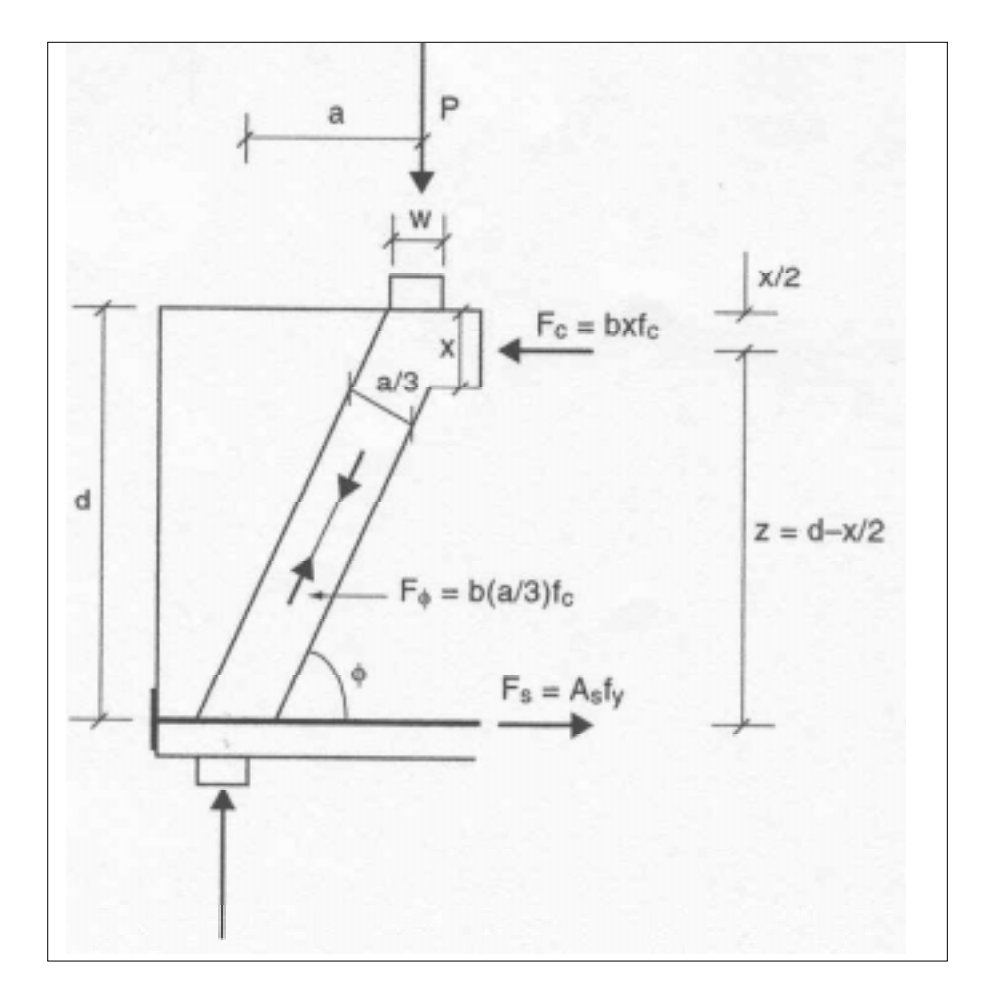


Figure 8: Assessment of load-carrying capacity of structural elements characterised by type IV behaviour: 1. Moment equilibrium requires  $F_c z = Pa$  which yields x; 2. Horizontal force equilibrium yields A; 3. Check whether a/3 satisfies the condition  $F\phi \sin \phi > P$  which prevents brittle failure (where  $\tan \phi = z/a$ ): if not, adjust b (breadth of beam) and repeat procedure. (Note: when the actual loaded width w is less than a/3 – this is unlikely to be the case in practice, but it often happens in beam testing -a/3 should be replaced by w).

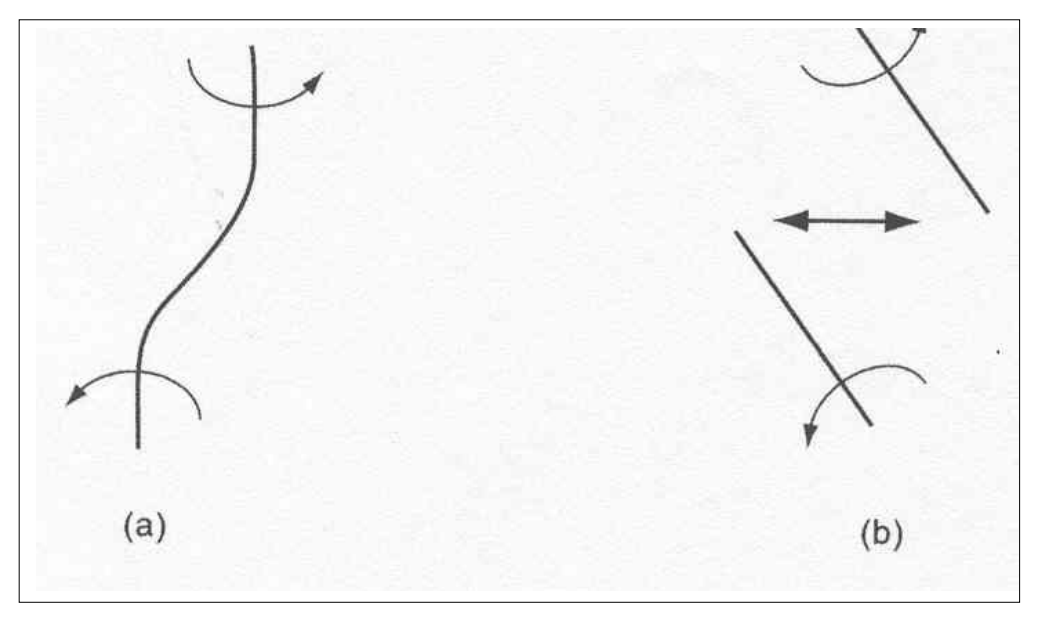


Figure 9: Beam (or beam-column) exhibiting a point of inflexion in a structure (a) and illustration of the internal tie needed at the point of contraflexure in order to prevent separation of the two ends of the member (b).

Finally, the formation of a fictitious internal support in the region of the point of contraflexure implies that concrete is locally subjected to a direct tensile, rather than shear, force causing failure when the tensile strength of the material is exceeded. This type of failure is prevented by specifying transverse reinforcement in a quantity sufficient to sustain the tensile force in excess of that which can be sustained by concrete alone. Such reinforcement is placed within the geometric locus of the point of contraflexure, and extends within a total length equal to the beam's depth d. Here, it is essential to appreciate that contraflexure is associated with the kind of response undergone by a beamcolumn in a building subjected to lateral sway (but applicable to any beam or frame with a point of contraflexure) as illustrated in Fig. 9: it is evident that the tie is needed to prevent separation of the ends of the member, and that the force in the tie is numerically equal to the shear force at the point of inflexion. It is significant that a survey of column and structural-wall failures in the aftermath of the 1999 Athens earthquake revealed that most of such failures (especially in the more recently constructed buildings which had been designed to modern codes) had in fact occurred at points of inflexion (Kotsovos and Pavlović 2001).

### 3. Examples

In what follows, several examples of the use of the CFP method for design are outlined, and their results are compared with the respective code predictions (as well as the experimental response of such systems when this is available). Clearly, these examples are not exhaustive but are intended to demonstrate the range of application of the proposed CFP methodology. Prior to these case studies, however, Fig. 10 illustrates – by reference to a specific instance of the generic structure depicted in Fig. 1 – the different detailing requirements of transverse reinforcement inherent in the TA and CFP approaches to design. The consequences of following such differing design philosophies will now be explored.

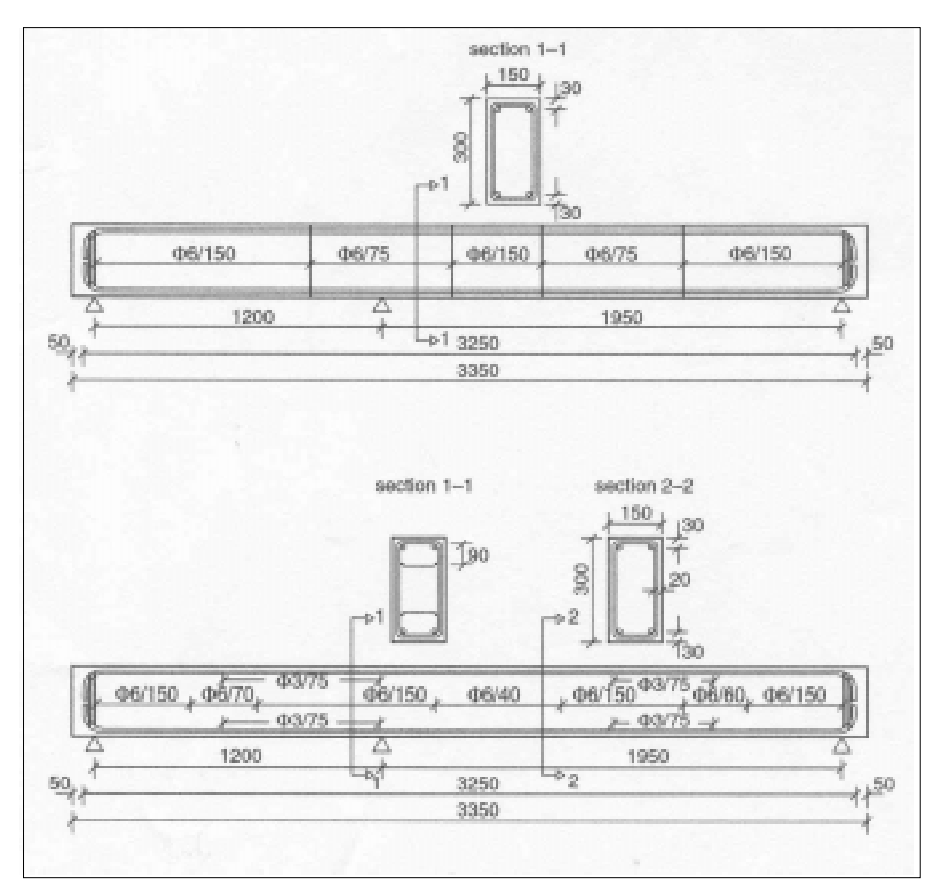


Figure 10: Design details of specimens shown in Fig. 1 (all dimensions in mm) designed to the TA (a) and to the CFP (b) philosophies – notice the different transverse-reinforcement requirements.

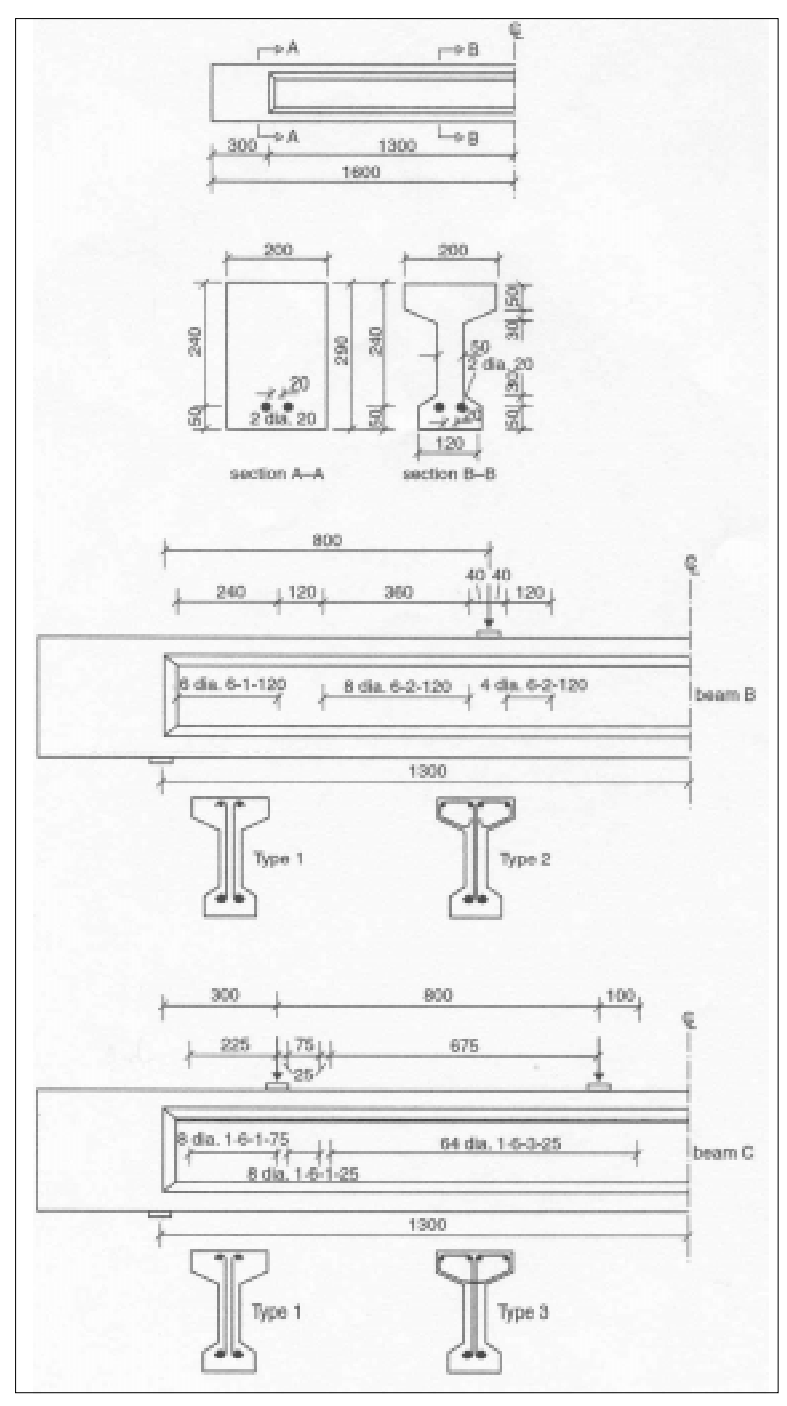


Figure 11: T-beams B and C (all dimensions in mm).

### Example 1: T-beams

Consider the simply supported Tbeams under two- and four-point loadings (denoted, respectively, as beams B and C), as illustrated in Fig. 11. Full design details (including material characteristics) are given by Kotsovos and Pavlović (1999). Their codepredicted load-carrying capacities (total load) are 148 kN (beam B) and 40 kN (beam C) because of the constraining shear-capacity clauses in current design methods (e.g. Comité Euro-International du Béton 1978; Technical Chamber of Greece 1991). On the other hand, their flexural capacities - which the CFP methodology (to which these girders were designed) predicts will be attained – are 182 kN (B) and 208 kN (C). When these members were tested experimentally, the total loads attained were, in actual fact,

191 kN (B) and 240 kN (C), implying a potential discrepancy (implicit in the code predictions) as high as 500% on the safe side (beam C). Moreover, while codes predict brittle types of failure, the observed failure modes in the tests were ductile, confirming the CFP designs: this is illustrated in. Figure 12, which depicts the test results for the two beams in terms of load-deflection curves, indicating also both code and CFP ultimate-load predictions. The results for a similar beam (designed and tested prior to beams B and C, and analysed by means of the NLFEM (Kotsovos and Pavlović 1995), appear in Fig. 13, showing the discrepancy between the FE analysis and test on the one hand, and the code predictions on the other hand (some of the latter predicting practically only onetenth of the true load attained).

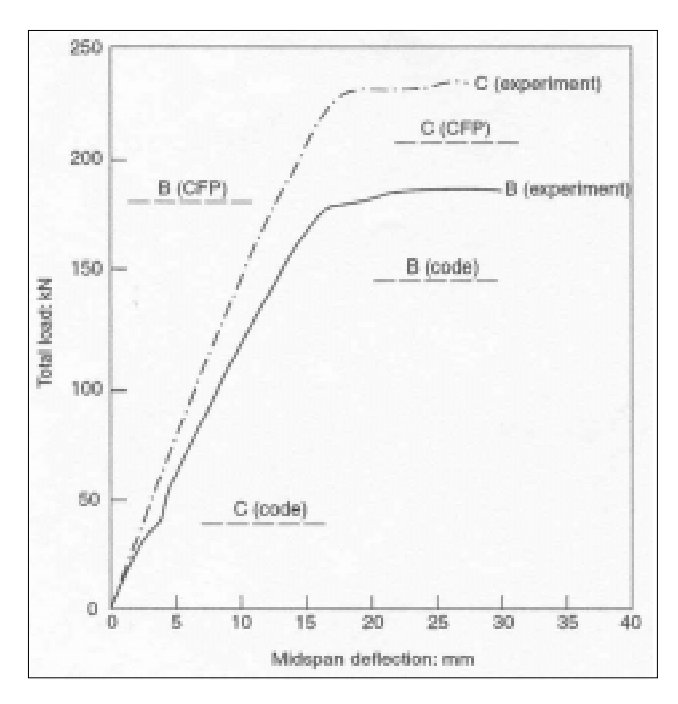


Figure 12: Experimental load-deflection curves for beams B and C (Fig. 11), with both code (e.g. CEB-FIP, TCG - see Kotsovos and Pavlovic 1999) and CFP predictions also shown.

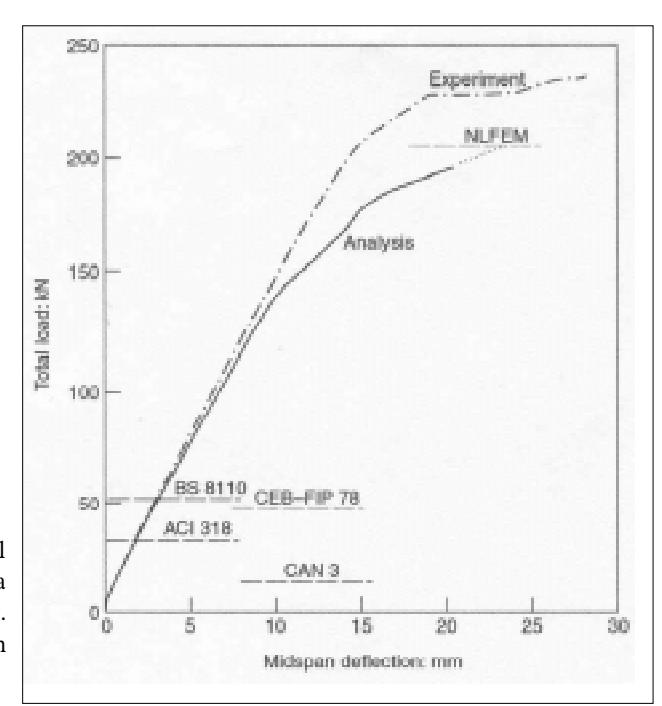


Figure 13: Experimental and numerical (NLFEM) load-deflection curves for a T-beam similar to those depicted in Fig. 11 (Kotsovos and Pavlović 1995), with various code predictions also shown.

# Example 2: Column design for seismic action

The type of column considered in this example has been used to investigate the validity of the earthquake-resistant design clauses of current codes of practice (such as, for example, the Greek version of EC2/EC8). At the same time, this structural element can also be employed to demonstrate the ability of the CFP methodology to yield solutions that satisfy the performance requirements of structural design (Kotsovos and Pavlović 1999).

The design details of two typical columns, one designed to the Greek version of EC2 and the other to the CFP methodology, are shown in Figs. 14 and 15,

respectively. The figures also show the loading arrangement used to introduce a point of contraflexure within the column length. Such a loading arrangement was considered to be more representative of the loading conditions developing in real frame-like structures where the formation of points of contraflexure is inevitable. It is interesting to note in the figures that, while the code specifies a denser stirrup arrangement at the column ends (subjected to the combined action of the largest bending moment and shear force), it is in the region of the point of contraflexure where the CFP methodology specifies a denser stirrup arrangement since such reinforcement is considered essential by this methodology for sustaining the direct

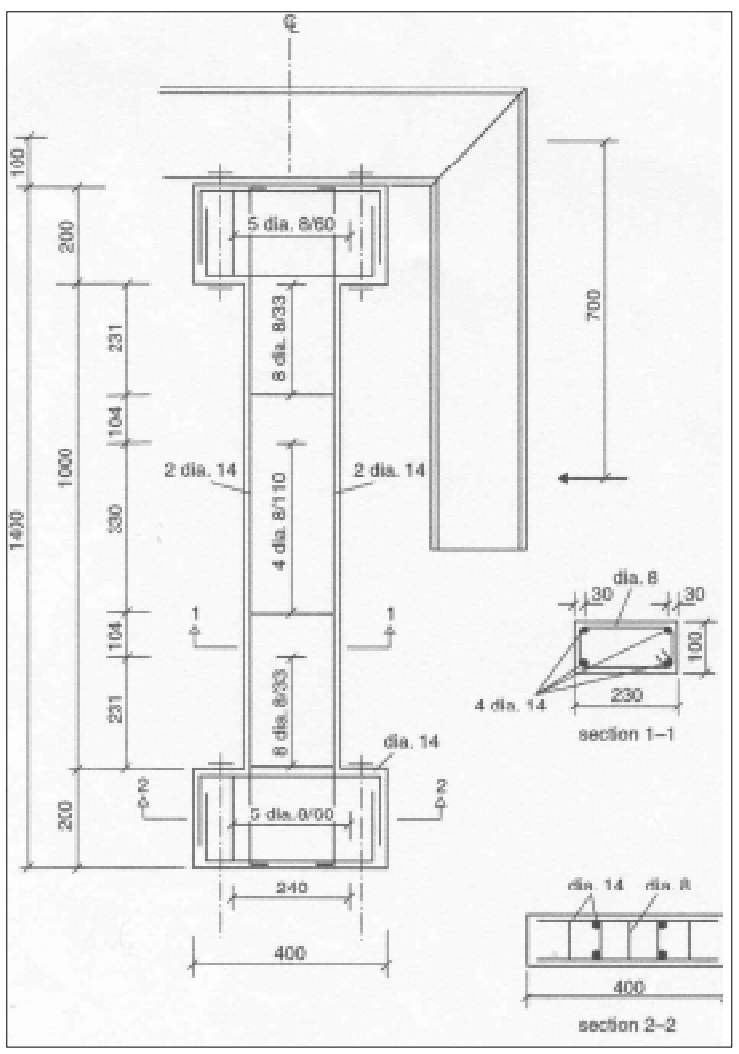


Figure 14: Design details and loading arrangement for column designed to the Greek version of the EC2 (all dimensions in mm).

tensile, rather than shear, force, which develops in this region. Full design details (including material characteristics) are given by Kotsovos and Pavlović (1999).

A schematic representation of the mode of failure of the column designed to the code, together with the bendingmoment and shear-force diagrams corresponding to the load-carrying capacity established experimentally as well as to the flexural capacity are shown in Fig. 16. The shear-force diagram in Fig. 16 also includes the code values of shear capacity at the middle and end zones of the column. The figure shows that the value of the horizontal load that caused failure

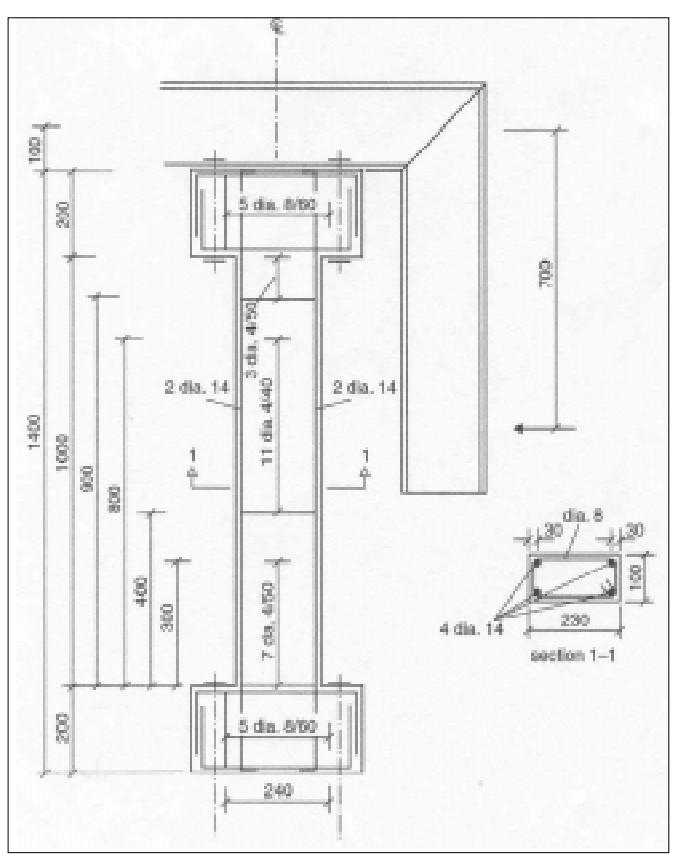


Figure 15: Design details and loading arrangement for column designed to the CFP methodology (all dimensions in mm).

of the column is 51.5 kN against the predicted value of 55.68 kN, i.e. the design prediction overestimates the true column load-carrying capacity by approximately 7%. Much more worrying, however, it should be noted that, while the prediction refers to flexural failure, the column failed in 'shear', in contrast with the code prediction for shear capacity corresponding to a load significantly larger than that causing flexural failure. It should also be noted that 'shear' failure occurred within the lower 'critical length' of the column

which was designed to the earthquakeresistant design clauses of the code, so as to have a shear capacity larger than that of the remainder of the column. In fact, as indicated in Fig. 16(b), the deviation of the value of 190 kN, predicted as shear capacity of the 'critical length', from the value of 51.5 kN established by experiment, is of the order of 260%.

The above deviation of the predicted from the experimentally established values is indicative of the inadequacy of the concepts which

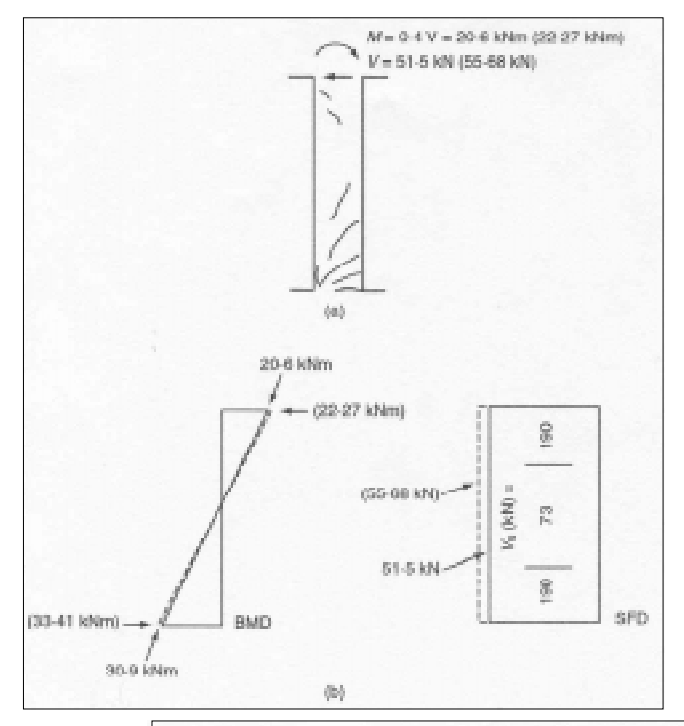


Figure 16: Experimental results for the column in Fig. 14: (a) schematic representation of crack pattern at failure; (b) bending-moment and shearforce diagrams corresponding to load-carrying capacity established experimentally (continuous lines) and flexural capacity (dashed lines) (the SFD also includes the code values of shear capacity at the various portions of the column).

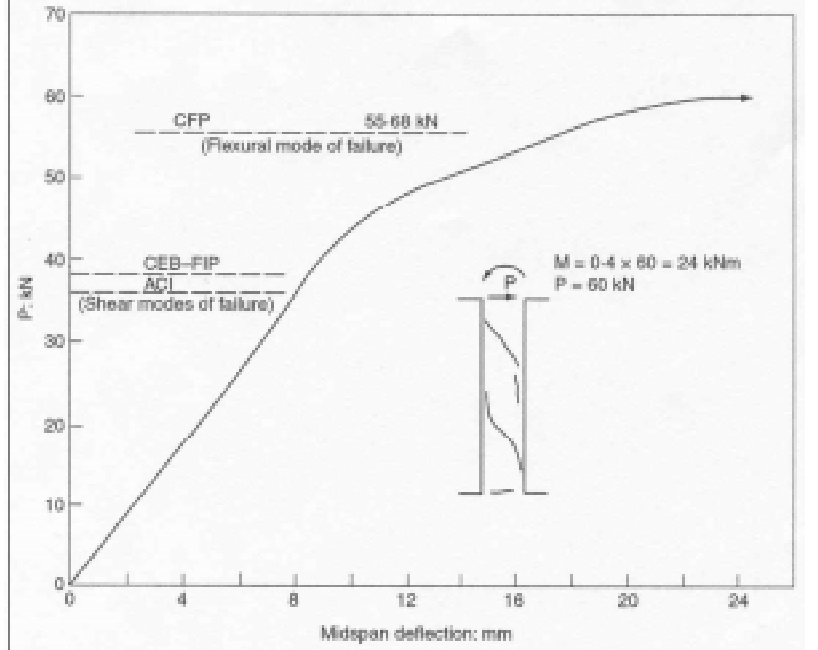


Figure 17: Experimental load-deflection curve for the column in Fig. 15, with the schematic representation of the crack pattern at failure and some code predictions.

underlie the earthquake-resistant structural-concrete design clauses of current codes of practice. The above clauses specify additional transverse reinforcement in 'critical lengths' of structural-concrete members, in excess of that required for safeguarding against 'shear' failure; the purpose of such additional reinforcement being not only to increase the margin of safety against 'shear' failure, but also to ensure ductility. And yet, the experimental information presented here demonstrates clearly that the increase in transverse reinforcement does not achieve either of the above two aims (i.e. improved strength and ductility) of structural design; in fact, it appears to cause a brittle, rather than the predicted ductile, mode of failure. An explanation for this has been given by Kotsovos and Pavlović (1999), showing that the tensile force recorded in the stirrups is so large that, instead of the stirrups contributing to carrying some of the shear force – as intended in present-day design and in accordance with the concepts underlying current code thinking – it appears that the reverse is true, namely the action of the stirrups seems to be resisted by the shear force sustained by concrete.)

In contrast with the column designed to the code, that designed to the CFP methodology achieved the aims of structural design for strength and ductility. This is illustrated in Fig. 17, which shows the load-deflection curve of the latter column, together with a schematic representation of the crack

pattern at failure, as well as the values of load-carrying capacity predicted by CFP and typical codes of practice. It is interesting to note in the figure that, for this case, the codes underestimate load-carrying capacity by a factor of nearly 2.

# Example 3: The failure of an offshore platform

One interesting instance of the application of the CFP methodology in practice has been its use for the investigation of the causes of failure of the structural wall element "tricell 23" which led to the collapse of the platform 'Sleipner 4' in the North Sea on August 23, 1991, prompting a recent interesting study reported by Collins et al. (1997). It was established that the collapse was due to the failure of the portion of the tricell wall, shown in Fig. 18, that did not contain stirrups; moreover, the failure of the above portion was found to have occurred not only because the magnitude of the shear force at the wall ends was underestimated by the global finite-element analysis performed but, also, because the benefits of axial compression on the wall's shear capacity were seriously overestimated by the sectional design procedure used. Furthermore, a comprehensive investigation of the response of RC wall elements combined axial in compression and shear demonstrated that, while ACI 318 (American Concrete Institute 1995) (which underlied the

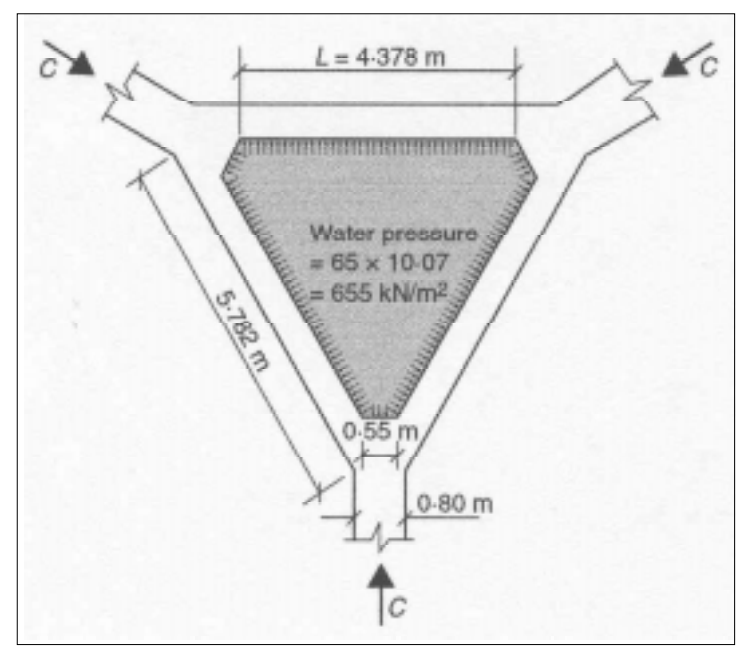


Figure 18: Details of the geometry and loading for the tricell wall 23 of the Sleipner 4 platform (reproduced from Collins et al. 1997).

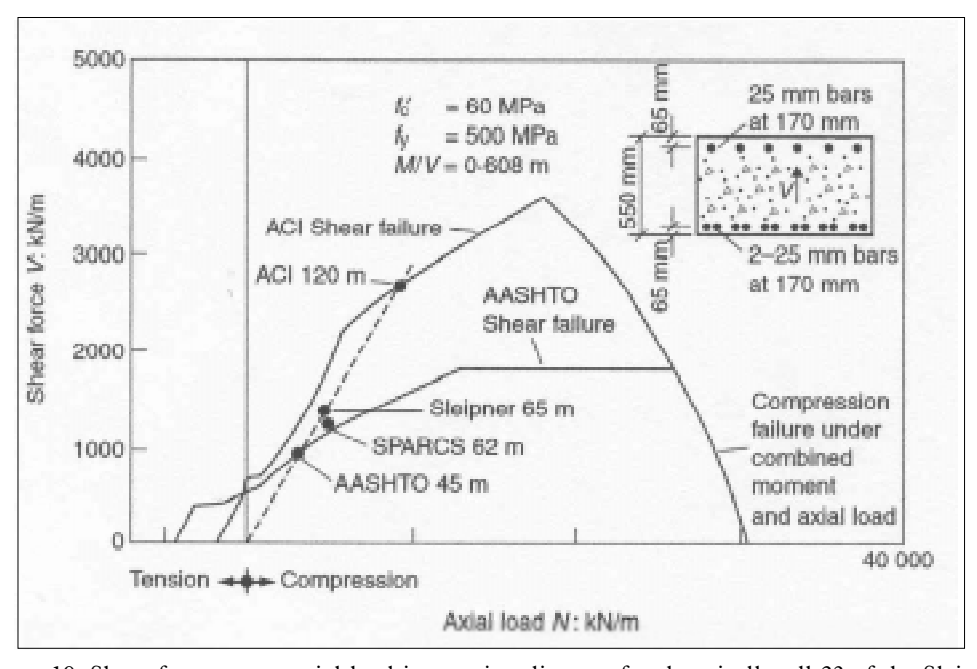


Figure 19: Shear force versus axial load interaction diagram for the tricell wall 23 of the Sleipner 4 platform (reproduced from Collins et al. 1997).

method used to assess the tricell-wall shear capacity) considerably overestimated shear capacity, AASHTO LRFD (American Association of State Highways and transportation Officials 1994) yielded more conservative as well as more accurate shear-capacity predictions.

From results of the experimental investigation reported by Collins et al. (1997), it appears that two additional interesting observations may be made. First, for the particular structural forms investigated, it is clear that, in spite of improved accuracy of the predictions, AASHTO does not always yield a close fit to experimental values, and, secondly, it is evident that failure of the specimens tested occurred in the middle portion of the walls, i.e. in the region of the point of inflexion, due to the formation of near-vertical cracking which occurred suddenly independently from the inclined cracking at the top end of the specimen where current codes predict shear capacity to be exhausted earlier than in other regions of the walls.

Kotsovos and Pavlović (1999) complemented the findings of Collins et al. (1997) by demonstrating that the use of the CFP concept can lead to close predictions of shear capacity while, at the same time, providing a realistic description of the causes of failure. Thus, the CFP technique was used to establish the ultimate limit-state characteristics of both the structural-wall elements tested by Collins et al.

(1997), as described in detail elsewhere (Kotsovos and Pavlović (1999), and the tricell wall component of the actual collapsed structure (as will presently be briefly outlined). The latter appears to have failed under the loading conditions described in Fig. 18 and 19.

For the geometric characteristics shown in Fig. 18 and 19, the flexural capacity of the end of the cross-section of the tricell wall (taken as a onemetre wide strip of the (one-way spanning) wall), in the presence of an axial force N satisfying the condition N/V=3.5 (where V is the shear force) imposed by the sinking operation (which also yields M/N = 208 mm, where M is the moment), can be easily assessed from first principles using the simplified stress block in Fig. 5 but allowing also for the presence of an axial force. Having established the flexural capacity (at the fixed-end cross-section) and the corresponding pressure (developing at a depth of approximately 168 m), it was easy to construct the internal force diagrams shown in Fig. 20 of which the bendingmoment diagram was then used for drawing the physical model of the tricell wall shown in Fig. 21. the latter figure it can be seen that the model comprises two end cantilevers, extending to the theoretical position of the point of contraflexure/ inflection situated at a distance of ~925 mm from the wall's ends, and a simply-supported beam covering the

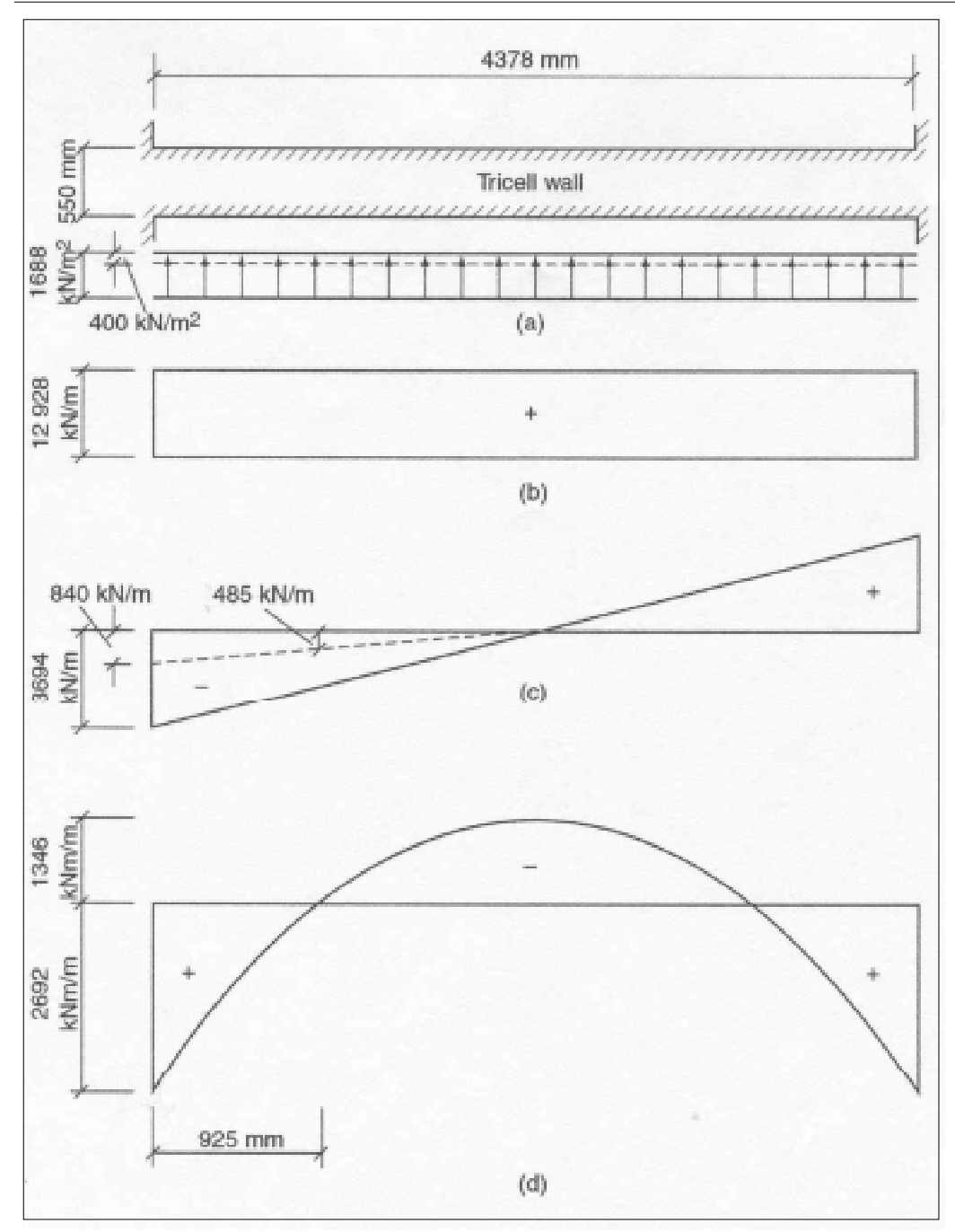


Figure 20: Hydrostatic pressure and internal-force diagrams for the tricell wall: (a) wall and acting pressure; (b) axial-force diagram; (c) shear-force diagram; (d) bending-moment diagram (note: continuous lines refer to flexural capacity, while the dashed lines correspond to some of the maximum predicted values).

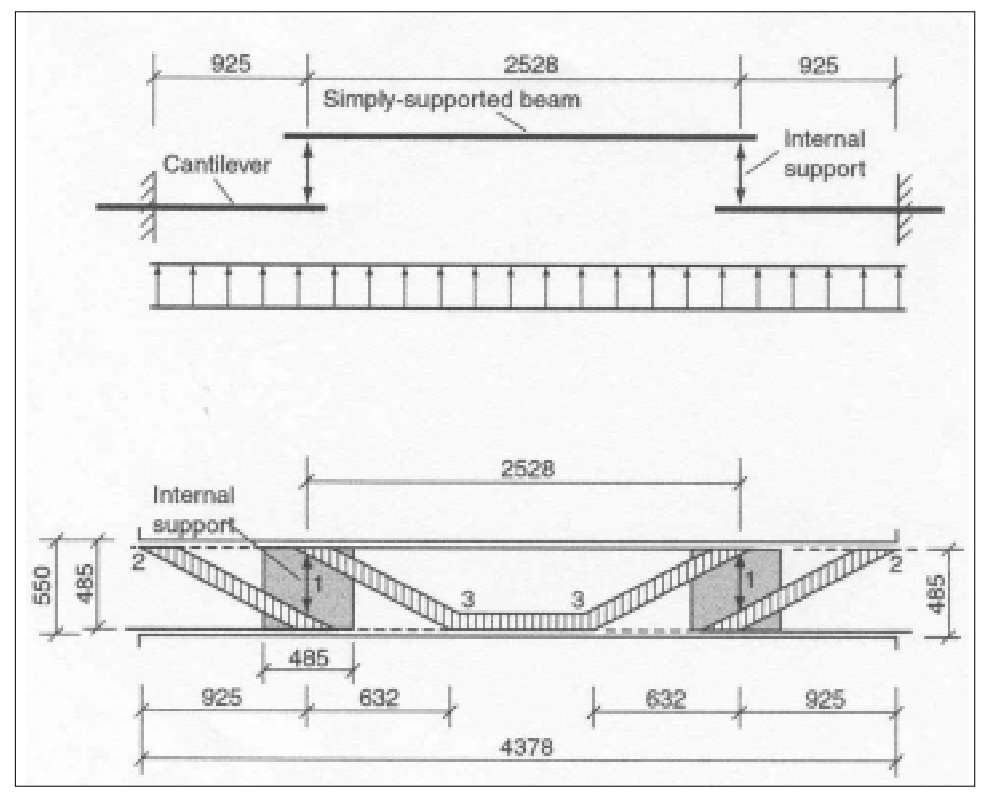


Figure 21: CFP model for the tricell wall (all dimensions in mm).

span between the cantilevers and being supported by them through an 'internal support' that, in the absence of transverse reinforcement, can only be provided by concrete.

Failure of the wall other than flexural may occur at the locations marked 1, 2 and 3 in Fig. 21. As explained earlier, the contribution of concrete to the formation of the internal support depends on the tensile strength of concrete which, for design purposes, is recommended to be given a value of 1 MPa (Kotsovos and Pavlović 1999). Hence, the total force that can be sustained by concrete in the region

of the point of inflection is f.bd =1x1000x485 = 485 kN, which is equivalent to the maximum value of shear force that can develop at the point of inflexion. From the shearforce diagram of Fig. 20, such a value of shear force at the location of the point of inflection corresponds to a shear force at the end of the wall equal to ~840 kN which develops under a pressure of ~400  $kN/m^2$  (i.e. at a depth of ~40m). It can easily be shown (Kotsovos and Pavlović 1999) that, in the absence of steel to form the 'tie' at the point of inflexion, this location 1 is critical as checks on the other

two locations of possible relevance (2 and 3) yielded higher loads. It would appear from the above, therefore, that the proposed method predicts that failure of the tricell wall was likely to have occurred at a depth as low as 40 m (and well below the depth of 168 m corresponding to flexural failure) owing to the failure of concrete (near-horizontal splitting parallel to the wall faces) in the region of the point of inflexion which lacked the requisite 'internal tie'.

### Example 4: Bridge assessment

In the United Kingdom there is an ongoing programme of checking whether or not road and railway bridges are capable of carrying 40 tonne loading in accordance with the Department of Transport document BD 21/01 (The Highways Agency 2001) which has superseded the earlier document BD 21/ 97 (The Highways Agency 1997). The number of bridges to be assessed is very large (running into tens of thousands) and the associated estimated costs of assessment and strengthening are in excess of £4bn (four billion pounds). The implications of traffic disruption and social inconvenience also implicit in the usually quite lengthy periods required to carry out what are deemed to be necessary strengthening works represent further factors which should be added to the above estimate.

The maximum bending-moment and shear-force values at the ultimate limit

state are traditionally computed using elastic methods (such as, for example, the grillage method). Member capacities are calculated using BD 44/95 (The Highways Agency 1995), which is a modified version of BS 5400 (British Standards Institution 1988). When comparing the calculated member capacities with the magnitudes of the applied bending and shear, some bridges theoretically fail to satisfy the assessment criteria in BD 21/01. And yet, site inspection usually reveals that the assessed bridges are adequate, showing no sign of cracking or distress. Of course, the reason why these bridges are not failing under the live load is because there is a reserve in the latent strength that could be exploited, and that the BD44/95 is too conservative. Accurate predictions of the true strength of concrete bridges are usually precluded by the fact that the analytical tools routinely employed are unreliable: for instance, it has been reported that, in the case of a short-span concrete bridge, elastic analysis constrained its "capacity" to 7.5t, a yield line program predicted a collapse load of 196t, while the actual full-scale load vielded "an enormous 367t" (Carcas 1998). It is the purpose of the present example to illustrate how a more rational assessment of the true strength of concrete bridges might lead to design solutions which will not only ensure safety but may well also result in large savings by avoiding unnecessary strengthening costs. Two case studies, drawn from existing bridges, are considered. Their full details have been

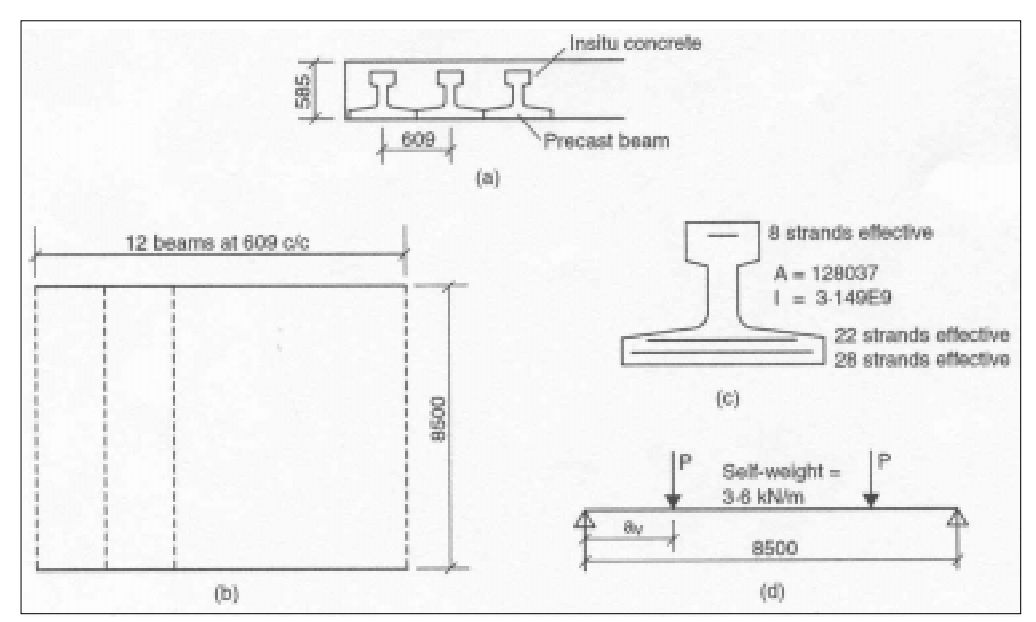


Figure 22: Deck type D: (a) elevation view; (b) plan view; (c) cross-section and reinforcement details; (d) loading configuration. Note: all dimensions are in mm (or mm², mm⁴ as appropriate).

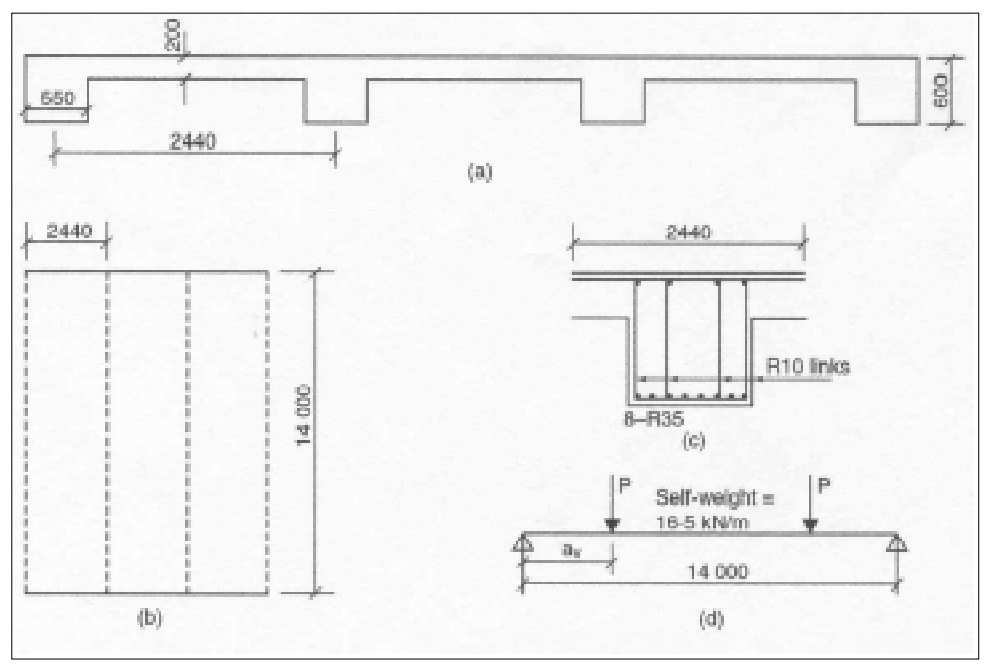


Figure 23: Deck type F: (a) elevation view; (b) plan view; (c) cross-section and reinforcement details; (d) loading configuration. Note: all dimensions are in mm.

reported elsewhere (Mahdi et al. 2003). Twopoint loading was assumed and various values of shear span were considered.

The first case study to be checked (deck type D) is a precast pretensioned beam. It forms part of a deck constructed using contiguous precast beams with solid infill. The main beam characteristics are shown in Fig. 22. Whereas BD 44/95 predicts a total load-carrying capacity (including self-weight) of 272 kN (based on shear capacity) irrespective of the value of shear span  $(a_n)$ , the CFP method shows that such a value is reasonably accurate only for length values of  $a_{x}$  (~ 1.75 m say) but that, for smaller  $a_{v}$ , serious underestimates of strength occur. For example, when  $a_n =$ 0.75 m, the CFP methodology predicts failure to take place when the total load reaches 734 kN, i.e. a 270% margin of safety is implicit in current standard calculations.

The second case study (deck type F) is a beam-and-slab girder, which, with the main properties of the resulting T-beam, are summarized in Figure 23. For this example, the total load-carrying capacity (including self-weight) in accordance with the BD 44/95 provisions (based, again, on shear capacity) is given as 660 kN when no links are present, and this value increases to 1184 kN when links (75 mm c/c) are introduced. On the other hand, and taking the case  $a_v = 0.710$  m, the CFP method guarantees an ultimate total load of 1800 kN irrespective of

whether or not links are present (since, in accordance to CFP calculations, flexural failure is attained in both cases so that additional stirrups (beyond the nominal shear reinforcement) will not result in higher load-carrying capacity). Again, one notices an underestimate of the true strength by code calculations which, in the absence of links, is of the order of 270%.

Tables 1 and 2 summarize the results for both bridge case studies, which encompassed three values of shear span for each structure. More formal results, obtained by means of the Authors' NLFEM (Kotsovos and Pavlović 1995) are also shown in these tables for purposes of comparison. It can be seen that both the complex NLFEM program and the much simpler CFP methodology yield similar results. Moreover, it is reassuring to note that the more basic hand calculations associated with the CFP technique provide safe estimates, as the CFP predictions are consistently slightly lower than their sophisticated NLFEM counterparts.

### 4. Conclusions

The CFP methodology (Kotsovos and Pavlović 1999) provides a simple alternative to the more fundamental approach of analysing concrete structures by means of formal three-dimensional modelling based on

triaxial behaviour and careful monitoring of crack propagation (Kotsovos and Pavlović 1995). Its simplicity is comparable to the type of calculations and checks in exciting codes of practice, and yet the accuracy provided by the CFP method in often far superior to that of its code counterparts, thus resulting in either potential savings or the avoidance of dangerously optimistic estimates. It is also interesting to note that that the CFP approach usually results in considerably less secondary reinforcement than that required by current design rules (an obvious exception is type III behaviour, where the CFP method specifies a larger amount of stirrups (to ensure additional moment capacity) than that resulting from code attempts to carry shear): however, the location and distribution of such CFP-derived transverse reinforcement differs radically from those of current practice. That a beam (if properly designed) prefers to act as a tied arch rather than a purely flexural member seems to have been understood by our Greek and Roman engineering predecessors, a fact confirmed by basic structural theory which states that the stiffer mode of structural action predominates. Such a concept can readily be extended to more complex structural systems by envisaging them as a chain of tied arches once they are properly "connected" at the locations of points of contraflexure.

#### References

American Association of State Highway and Transportation Officials (1994). AASHTO LRFD Design Specifications and Commentary. AASHTO.

American Concrete Institute (1995). *Building Code Requirements for Structural Concrete*. ACI 318-95.

American Concrete Institute (2002). *Building Code Requirements for Structural Concrete*. ACI 318-02.

Barnard, P.R. (1964). Researches into the complete stress-strain curve for concrete. *Mag. Concrete Res.*, v. 19, n. 49, p. 203-210.

Bobrowski, J. and Bardham-Roy, B.K. (1969). A method for calculating the ultimate strength of reinforced and prestressed concrete beams in combined flexure and shear. *The Structural Engineer*, v. 47, n. 5, p. 197-205.

British Standards Association (1988). Steel, Concrete and Composite Bridges. BS 5400.

Canadian Standards Association (1984). *Design of Concrete Structures for Buildings*. CAN3-A23.3-M84.

Carcas, R. (1998). *Verulam* correspondence ("Safety of bridges"), *The Structural Engineer*, v. 76, n. 2, p. 36.

Collins, M.P. and Mitchell, D. (1980). Shear and torsion design of prestressed and non-prestressed concrete beams. *PCI*, v. 25, n. 5, p. 32-100.

Collins, M.P.; Vecchio, F.J.; Selby, R.G. and Gupta, P.R. (1997). The failure of an offshore platform. *Concrete International*, February, p. 28-35.

Comité Euro-International du Béton (1978). *Model Code for Concrete Structures*. CEB-FIP.

Comité Européen de Normalisation (1991). Eurocode No. 2. Design of Concrete Structures. Part 1: General Rules and Rules of Building. ENV-1992-1. Comité Européen de Normalisation (1994). Eurocode No. 8. Design Provisions for Earthquake Resistance of Structures. ENV-1998-1-4.

Fenwick, R.C. and Paulay, T. (1968). Mechanisms of shear resistance of concrete beams. *J. Struct. Div.*, *Proc ASCE*, v. 94, n. ST10, p. 2325-2350.

González Vidosa, F.; Kotsovos, M.D. and Pavlović, M.N. (1991a). Three-dimensional nonlinear finite-element model for structural concrete. Part 1:main features and objectivity study. *Proc. ICE*, *Part* 2, v. 91, n. 3, p. 517-544.

González Vidosa, F.; Kotsovos, M.D. and Pavlović, M.N. (1991b). Three-dimensional nonlinear finite-element model for structural concrete. Part 2: generality study", *Proc. ICE*, *Part 2*, v. 91, n. 3, p. 545-560.

Hansford, M. (2002). Seismic codes oversimplified and unsafe. *New Civil Engineer*, 8/15 August, 28. (Report on Seminar by V. Bertero organized jointly by ICE Society for Earthquake & Civil Engineering Dynamics and Wessex Institute of Technology.)

Jan Bobrowski & Partners (progetto strutturale) and Graham McCourt (progetto architettonico) (1984). Il 'Saddledome': stadio olimpico del ghiaccio a Calgary (Canada). L'Industria Italiana del Cemento, n. 5.

Jelić, I.; Pavlović, M.N. and Kotsovos, M.D. (1999). A study of dowel action in reinforced concrete beams. *Mag. Concrete Res.*, v. 51, n. 2, p. 131-141.

Kani, G.N.J. (1964). The riddle of shear and its solution. *J. ACI (Proceedings)*, v. 61, n. 4, p. 441-467.

Kotsovos, M.D. (1979). Fracture of concrete under generalized stress. *Materials & Struct.*, *RILEM*, v. 12, n. 72, p. 151-158.

Kotsovos, M.D. (1983). Effect of testing techniques on the post-ultimate behaviour of concrete in compression. *Materials & Struct.*, *RILEM*, v. 16, n. 91, p. 3-12.

Kotsovos, M.D. (1987). Shear failure of reinforced concrete beams. *Eng. Struct.*, v. 9, n. 1, p. 32-38.

Kotsovos, M.D. and Newman, J.B. (1981). Fracture mechanics and concrete behaviour. *Mag. Concrete Res.*, v. 33, n. 115, p. 103-112.

Kotsovos, M.D. and Pavlović, M.N. (1986). Non-linear finite-element modelling of concrete structures: basic analysis, phenomenological insight, and design implications. *Eng. Computations*, v. 3, n. 3, p. 243-250.

Kotsovos, M.D. and Pavlović, M.N. (1995). Structural concrete: finite-element analysis for limit-state design. Thomas Telford, London.

Kotsovos, M.D. and Pavlović, M.N. (1999). *Ultimate limit-state design of concrete structures: a new approach*. Thomas Telford, London.

Kotsovos, M.D. and Pavlović, M.N. (2001). The 1999 Athens earthquake: causes of damage not predicted by structural concrete design methods. *The Structural Engineer*, v. 79, n. 15, p. 23-29.

Mahdi, A.A.; Kotsovos, M.D. and Pavlović, M.N. (2003). Towards a more rational approach for assessing and rating concrete bridges. *Proceedings of the 10<sup>th</sup> International Conference (Structural Faults and Repair – 2003)*, 1-3 July, London, 13 pages (on CD-ROM).

Mörsch, E. (1902). Versuche über Schubspannungen in Betoneisentragen. *Beton und Eisen*, v. 2, n. 4, p. 269-274.

Priestley, M.J.N. (1997). Myths and fallacies in earthquake engineering: conflicts between design and reality. *Concrete International*, February, p. 54-63.

Ritter, W. (1899). Die Bauweise Hennebique. *Schweisserische Bauzeitung*, v. 33, p. 59-61.

Schlaich, J.; Schafer, K and Jennewein, M. (1987). Toward a consistent design of structural concrete. *PCI*, v. 32, n. 3, p. 74-150.

Taylor, H.P.J. (1969). Investigation of the dowel shear forces carried by tensile steel in reinforced concrete beams. *Technical Report 431* (*Publication 42.431*), C&CA.

Taylor, H.P.J. (1974). The fundamental behaviour of reinforced concrete beams in bending and shear. *ACI Publication SP-42*, ACI, p. 43-77.

Technical Chamber of Greece (1991). Code of Practice for the Design and Construction of Reinforced Concrete Structures. TCG (in Greek).

The Highways Agency (1995). *The Assessment of Concrete Highways and Structures*. BD 44/95.

The Highways Agency (1997). The Assessment of Highway Bridges and Structures. BD 21/97.

The Highways Agency (2001). The Assessment of Highway Bridges and Structures. BD 21/01.

van Mier, J.G.M. (1986). Multiaxial strainsoftening of concrete. *Materials & Struct.*, *RILEM*, v. 19, n. 111, p. 179-200.

van Mier, J.G.M.; Shah, S.P.; Arnaud, M.; Balayssac, J.P., Bascoul, A.; Choi, S.; Dasenbrock, D.; Ferrara, G.; French, C.; Gobbi, M.E.; Karihaloo, B.L.; Konig, G.; Kotsovos, M.D.; Labuz, J.; Lange-Kornbak, D., Markeset, G., Pavloviæ, M.N., Simsch, G., Thienel, K-C., Turatsinze, A.; Ulmer, U.; van Geel, J.G.M.; van Vliet, M.R.A. and Zissopoulos, D. (1997). Strainsoftening of concrete in uniaxial compression. *Materials & Struct.*, *RILEM*, v. 30, n.198, p. 195-209. (Report of the Round Robin Test carried out by RILEM TC 198-SSC: Test methods for the strain-softening response of concrete).